Research Article

Marwa A. A. Fayed, Lamya H. Al-Wahaibi*, Riham O. Bakr, Mai S. Nour, Omer A. Basudan, Mohammad K. Parvez, Mohammed S. Al-Dosari, Wael M. Abdel-Mageed*

Sterols from *Centaurea pumilio* L. with cell proliferative activity: *In vitro* and *in silico* studies

https://doi.org/10.1515/chem-2022-0316
received February 22, 2023; accepted April 2, 2023

Abstract: Numerous studies highlighted the impact of natural products, particularly phytosterols, in wound healing while providing less expensive alternatives to chemically synthesized drugs, with less side effects. *Centaurea pumilio* L. (family Asteraceae) is a rare and endangered species of genus *Centaurea* with few reports concerning its chemistry. Our phytochemical investigation for the non-polar fraction of its aerial parts led to the isolation and identification of the new compound (**6**) identified as stigmast-1,5-dien-3-*O*-β-D-glucopyranoside along with five known sterols and triterpenes (**1–5**) identified as taraxasterol, β-sitosterol, stigmasterol, β-sitosterol glucoside, and stigmasterol-3-*O*-β-D-glucopyranoside. Structures of the isolated compounds have been characterized using 1D, 2D NMR, and mass spectral analyses. The cell viability and proliferative activity of the isolated compounds were evaluated using an MTT assay on cultured human primary umbilical vein endothelial cells (HUVEC). None of the compounds exhibited any sign of cytotoxicity. Nonetheless, compounds **5** and **6** moderately enhanced the HUVEC cell growth by 14 and 16%, respectively, at the maximal tested dose (50 μg/mL). As inhibition of glycogen synthase kinase 3-β (GSK3-β) enzyme is important to enhance the wound healing process; therefore, molecular docking was performed to understand the possible interactions between bioactive compounds **5** and **6** and GSK-3β binding pocket active amino acid residues. Both compounds were able to bind to the substrate-binding site of GSK-3β and potentially interact with the key active site residues, forming strong π and hydrogen interactions with the catalytic site residues, revealing lower binding energy (−7.185 and −6.303 kcal/mol, respectively) than that of indirubin-3-monooxime (−5.303 kcal/mol); thereby representing strong natural replacements candidates for GSK-3β inhibitors.

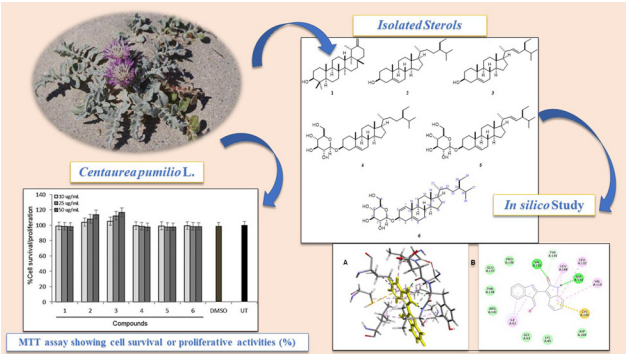

Graphical abstract

Keywords: *Centaurea pumilio*, sterols, triterpenes, HUVEC, growth stimulatory activity

1 Introduction

Phytosterols have been attracting the attention of researchers for years because of their important hypercholesteremic,

* **Corresponding author: Lamya H. Al-Wahaibi,** Department of Chemistry, Science College, Princess Nourah Bint Abdulrahman University, Riyadh, Saudi Arabia, e-mail: lhalwahaibi@pnu.edu.sa
* **Corresponding author: Wael M. Abdel-Mageed,** Department of Pharmacognosy, College of Pharmacy, King Saud University, P.O. Box 2457, Riyadh 11451, Saudi Arabia; Pharmacognosy Department, Faculty of Pharmacy, Assiut University 71526, Assiut, Egypt, e-mail: wabdelmageed@ksu.edu.sa
Marwa A. A. Fayed: Department of Pharmacognosy, Faculty of Pharmacy, University of Sadat City, Sadat 32897, Egypt, e-mail: marwa.fayed@fop.usc.edu.eg
Riham O. Bakr: Department of Pharmacognosy, Faculty of Pharmacy, October University for Modern Sciences and Arts (MSA), 11787, Giza, Egypt, e-mail: romar@msa.edu.eg
Mai S. Nour: Department of Pharmaceutical Chemistry, Faculty of Pharmacy, October University for Modern Sciences and Arts (MSA), 11787, Giza, Egypt, e-mail: msaeed@msa.edu.eg
Omer A. Basudan: Department of Pharmacognosy, College of Pharmacy, King Saud University, P.O. Box 2457, Riyadh 11451, Saudi Arabia, e-mail: basudan@ksu.edu.sa
Mohammad K. Parvez: Department of Pharmacognosy, College of Pharmacy, King Saud University, P.O. Box 2457, Riyadh 11451, Saudi Arabia, e-mail: mohkhalid@ksu.edu.sa
Mohammed S. Al-Dosari: Department of Pharmacognosy, College of Pharmacy, King Saud University, P.O. Box 2457, Riyadh 11451, Saudi Arabia, e-mail: mdosari@ksu.edu.sa

anticancer, anti-inflammatory, and antioxidant effects, along with their potential efficacy for treating cardiovascular diseases [1]. They are plant-derived fatty compounds representing the most prominent part of unsaponifiable matter found in all plant foods [1]. They are referred to as "plant cholesterol" because of their structural similarity to cholesterol, as they mainly differ in the side chain. An additional double bond at the C-22 position (brassicasterol or stigmasterol), or an ethyl (sitosterol) or a methyl group (campesterol) at the C-24 position differentiates them from cholesterol [2]. Within phytosterols, β-sitosterol, campesterol, and stigmasterol are the major phytosterols that account for about 65, 30, and 3% of human herbal nutrition, respectively [3].

Wound healing involves many processes, including cellular infiltration, inflammation, and proliferation [4]. The most significant protein involved in these processes is glycogen synthase kinase 3 (GSK-3), which is involved in the well-known Wnt/β-catenin and is crucial for activities such as cell division and wound healing [5]. According to several studies, inhibiting this protein speeds up wound healing [6,7]. As chemically derived treatments are commonly expensive and come with major side effects, natural wound healing agents are being increasingly researched.

Centaureinae is the largest subtribe in the family Asteraceae, and it comprises many plant genera, including the genus *Centaurea*, which comprises about 500 species. Phytochemical investigations have shown that acetylenes, flavonoids, lignans, and sesquiterpene lactones, which form the principal class of phytoconstituents, are abundant in species belonging to this subtribe [8–10]. Sterols and/or triterpenes have also been identified in many species, including *Centaurea* species [11–13].

Centaurea pumilio L. (*Aegialophila pumilio* L. Boiss) is a rare and endangered species mainly scattered on the deltaic Mediterranean coast in Egypt and throughout the Mediterranean coast [14]. Data on the phytoconstituents of *C. pumilio* are scarce, and only flavonoids identified in its leaf methanolic extract [15] besides phenolic and fatty acids identified from callus methylene chloride and ethyl acetate extracts using UPLC-ESI-MS/MS analyses [16].

Additionally, its essential oil showed the presence of sesquiterpene hydrocarbons in which the major constituent was β-caryophyllene (29.33%), followed by isogermacrene D (17.28%), besides the identification of caryophyllene oxide, α-humulene, α-copaene, γ-elemene, and T-muurolol [17]. Biological studies have shown significant antimicrobial activity of its essential oil [17], in addition to antioxidant, whitening, anti-aging, and schistosomicidal effects [15,18].

In continuation of our ongoing research activities toward the isolation of chemical constituents from wild plants growing in Egypt, we extended our investigation to the aerial parts of *C. pumilio*. Herein, we reported the isolation and structural elucidation of five sterols and one triterpene (**1–6**) from *C. pumilio* for the first time, including one new compound, namely stigmast-1,5-dien-3-*O*-β-D-glucopyranoside (**6**), isolated from the non-polar fraction. In addition, the proliferative effects of the isolated compounds were investigated on human umbilical vein endothelial cells (HUVECs) accompanied by assessing *in silico* binding affinity against glycogen synthase kinase-3 β (GSK-3 β) to understand their action mechanisms.

2 Materials and methods

2.1 Plant material

The aerial parts of *C. pumilio* were collected in August 2017 in Burg El-Arab, Alexandria province, Egypt. Prof. A.A. Fayed, who is a professor of Plant Taxonomy at the Faculty of Science, Assiut University, Assiut, Egypt, kindly identified the plant. A voucher sample (alphabetically ordered under the letter "*C*") was deposited in the herbarium of the Faculty of Science, Assiut University. The collected parts were cleaned, dried, and crushed into a coarse powder.

2.2 General experimental procedures

The 1D and 2D NMR spectroscopy experiments were carried out using the UltraShield Plus system (Bruker Biospin GmbH, Rheinstetten, Germany) operating at 500 MHz for ^{1}H and 125 MHz for ^{13}C. High-resolution electron ionization mass spectrometry (HR-EI-MS) was carried out using a Bruker microTOF mass spectrometer. Moreover, JASCO 320-A spectrometers and Perkin-Elmer Model 343 polarimeters were used to measure optical rotations and IR spectra, respectively; 230–400 mesh ASTM silica gel (Merck 60 A, Darmstadt, Germany) was used for normal-phase column chromatography whilst thin-layer chromatography (TLC) was performed on normal-phase silica gel (Merck, Darmstadt, Germany), with an average particle size of 10–12 m, 250 m layer thickness and utilizing different solvent systems, including *n*-hexane:EtOAc, *n*-hexane:DCM, DCM:EtOAc, and DCM:MeOH. Additionally, the compounds were visualized by spraying the TLC plates with 10% H_2SO_4/ethanol, followed by heating. All the chemicals and solvents used were of analytical grade.

2.3 Extraction and isolation

The dried powdered aerial parts of *C. pumilio* (500 g) were extracted sequentially with dichloromethane (3 × 1.5 L) and then methanol (3 × 1.5 L), by maceration until fully consumed. The filtrates were then collected and concentrated separately on a rotary evaporator (Heidolph, Germany) at 40°C, yielding 17 and 44 g of the dichloromethane (DCM) and methanol extracts, respectively. In the previous study, the methanolic extract was subjected to conventional column chromatography resulting in the isolation and identification of eight phenolic compounds besides the tentative identification of twenty-nine different phytoconstituents [15]. In this study, the dichloromethane extract was the subject of phytochemical and biological analysis to investigate its active constituents and their potential biological activities.

The DCM extract (17 g) was chromatographed by column chromatography on silica gel (Merck 60 A, 230–400 mesh), utilizing gradient elution with DCM:ethyl acetate as the mobile phase. Similar fractions were blended and concentrated at lower pressure based on the TLC to produce eight major fractions (CPC-I through CPC-VIII). In general, the fractions were viewed under a UV lamp with a wavelength of 254–366 nm, sprayed with 10% H_2SO_4 in ethanol, and then heated to 120°C. Subfraction CPC-II (3 g) was re-chromatographed on a silica gel column (120 g), utilizing gradient elution with DCM:EtOH as a mobile phase to elute it. TLC was used to track and combine similar 20 mL fractions. Compound (**1**) (30 mg) was obtained from the fractions eluted with DCM:EtOH (9.5:0.5), whereas compounds (**2**) (21 mg) and (**3**) (32 mg) were obtained from the fractions eluted with DCM: EtOH (9:1). Sub-fraction CPC-V (2.5 g) was re-chromatographed on a silica gel column (100 g), and the gradient elution of a DCM:EtOH mixture was used to elute it. The fractions (20 mL each) were collected and monitored by TLC. Compound (**4**) (18 mg) was obtained from fractions eluted with DCM:EtOH (8:2), whereas compounds (**5**) (27 mg) and (**6**) (25 mg) were obtained from fractions eluted with DCM:EtOH (7:3).

2.4 Phytochemical screening

A qualitative analysis of the recently obtained crude extract of *C. pumilio* flowering aerial parts was conducted. Using established methods, the presence of phytochemicals belonging to different classes was detected by distinctive color changes.

2.4.1 Detection of alkaloids (Dragendorff's test)

About 0.1 mL of the methanolic extract was mixed with Dragendorff's reagent, and the resulting orange-red precipitate confirmed the presence of alkaloids [19].

2.4.2 Detection of triterpenoids and/or steroids (Salkowski's test)

Chloroform (2 mL) mixed with the total extract was combined with a few drops of concentrated sulfuric acid. The presence of triterpenes and/or steroids was indicated by a reddish-brown coloring [19].

2.4.3 Detection of anthraquinone glycosides (modified Bontrager's test)

Using diluted hydrochloric acid, the extract was hydrolyzed; 5 mL of chloroform was added after filtering, and the mixture was agitated. After decantation, the chloroform phase was evaporated until dry. Two milliliters of diluted ammonia was added to the residual. After heating in the water bath, a yellow color that did not turn red indicated the absence of anthraquinone glycosides [20].

2.4.4 Detection of cardiac glycosides (Baljet's test)

Each total extract that had been filtered (1 mL) was pretreated with lead acetate (1 mL). The filtrate was combined with sodium hydrogen phosphate, filtered, and mixed with Baljet's reagent to produce red–orange cardenolides [21].

2.4.5 Detection of saponins (froth test)

The total extract (2 mL) and 2 mL of distilled water were forcefully shaken. After 5 min of stirring, the presence of froth was used to confirm the presence of saponins [19].

2.4.6 Detection of tannins and phenolics ($FeCl_3$ test)

The total extract (50 mg) was diluted in 5 mL of distilled water, and a few drops of $FeCl_3$ were added. The development of a blue-green or black tint indicated the presence of tannins and phenolic constituents [20].

2.4.7 Detection of flavonoids

One milliliter of the whole methanolic extract was combined with a few drops of KOH (5%) to produce a bright yellow hue as opposed to the blank. By adding diluted HCl, the color was rendered inert, confirming the presence of flavonoids [20].

2.4.8 Detection of coumarins

After evaporating the whole amount of ethanolic extract (2 mL), the residue was dissolved in hot distilled water (2 mL), after which it was split into two equal portions. The first component served as a blank, and 0.5 mL of 10% NH_4OH was added to the second. A drop of each solution was placed on filter paper, and the drops were then analyzed using a UV light. The observed bright fluorescence of the drop belonging to the second component indicated the presence of coumarins [19].

2.4.9 Detection of reducing sugars

One milliliter of an ethanol extract and 20 drops of boiling Fehling's solution (A and B) were mixed with 1 mL of water in a test tube. The presence of reducing sugars was indicated by the formation of a precipitating red brick at the bottom of the tube [22].

2.5 Biological studies

To test the cytotoxicity of the extracted compounds as well as their effects on cell viability, human primary umbilical vein endothelial cells (HUVEC) were cultivated in the DMEM-Glutamax medium with 10% bovine calf serum and 1× penicillin–streptomycin (Invitrogen, USA) at 37°C with 5% CO_2. One day before the experiment, HUVEC cells (0.5×10^5 cells/100 µL/well) were sown in a 96-well culture plate (Becton-Dickinson Labware, USA) and cultured overnight. Stocks of all six compounds were prepared by first dissolving them in 50 µL DMSO (Sigma, Germany), followed by reconstitution in DMEM (1 mg/mL, final). Further, for each compound, five working concentrations (2, 5, 10, 25, and 50 µg/mL) were prepared in DMEM. Notably, the final concentration of DMSO in the treatment doses never exceeded 0.1%. The cells were treated with each compound (triplicated dose) and DMSO (0.1%; vehicle control), along with untreated control, and incubated for 72 h.

The cell viability or proliferation was assessed using MTT (TACS MTT Cell Proliferation and Viability Assay Kit) as per the manufacturer's instructions. In a 96-well culture plate, an MTT reagent (10 µL/well) was added to each well and incubated for 4 h in the dark at room temperature, followed by the addition of a detergent solution (100 µL/well) and incubation for 1.5 h at 37°C. The microplate reader (ELx800; BioTek, USA) was used to measure the absorbance at λ = 570 nm. Using Excel (Microsoft, USA), the data were analyzed for percent cell survival or proliferation in comparison with the untreated control using the following equation: $(A_s - A_b)/(A_c - A_b)] \times 100$, where A_s, A_b, and A_c represent the absorbance of sample, blank, and negative control, respectively. The experiment was performed with triplicated samples and repeated twice for reproducibility.

2.6 Molecular docking

The interaction between the most potent compounds (**5**) and (**6**) and the active site of GSK-3β (PDB code: 1Q41) was elucidated by performing molecular docking using Autodock 4.2 [23]. The crystal structure, retrieved from a protein databank (https://www.rcsb.org/pdb), in complex with indirubin-3-monooxime as a native ligand, was prepared using Autodock tools [23]. Before molecular docking, water molecules were removed from the protein structure, and then, the partial charges were assigned using Gasteiger charges to the protein structure, as well as to the ligands.

The active site was defined using a grid box centered on the native ligand with dimensions of 30 × 30 × 30 points and a spacing of 0.375 Å. For each compound, 100 docking runs were conducted using the Lamarckian genetic algorithm in the default Autodock parameters [23]. Visualization was achieved using a discovery studio [24]. Validation was performed by redocking the native ligand, identifying the amino acids involved, and ligand interactions with the active site amino acids were studied.

3 Results and discussions

3.1 Preliminary phytochemical analysis

The phytochemical analysis of the total methanolic extract of *C. pumilio* aerial parts revealed the absence of anthraquinones and cardiac glycosides and the presence of

Table 1: Preliminary phytochemical screening of the total alcohol extract of *C. pumilio* L. aerial parts

S. No.	Preliminary phytochemical tests	Test name	Results
1	Test for steroids and/or triterpenoids	Salkowski's test	+
2	Test for flavonoids	Alkali test	+
3	Test for anthraquinone glycosides	Modified Bontrager's test	–
4	Test for cardiac glycosides	Baljet's test	–
5	Test for alkaloids	Dragendorff's test	+
6	Test for tannins and phenolics	$FeCl_3$ test	+
7	Test for saponins	Frothing test	+
8	Test for coumarins	Fluorescent test	+
9	Test for reducing sugars	Fehling's test	+

+ = presence; – = absent.

several phytoconstituent classes, including steroids and/or triterpenes, flavonoids, alkaloids, tannins, saponins, coumarins, polyphenolics, and reducing sugars, as summarized in Table 1.

3.2 Characterization of isolated compounds

The dried aerial parts of *C. pumilio* (500 g) were progressively extracted by maceration at room temperature until

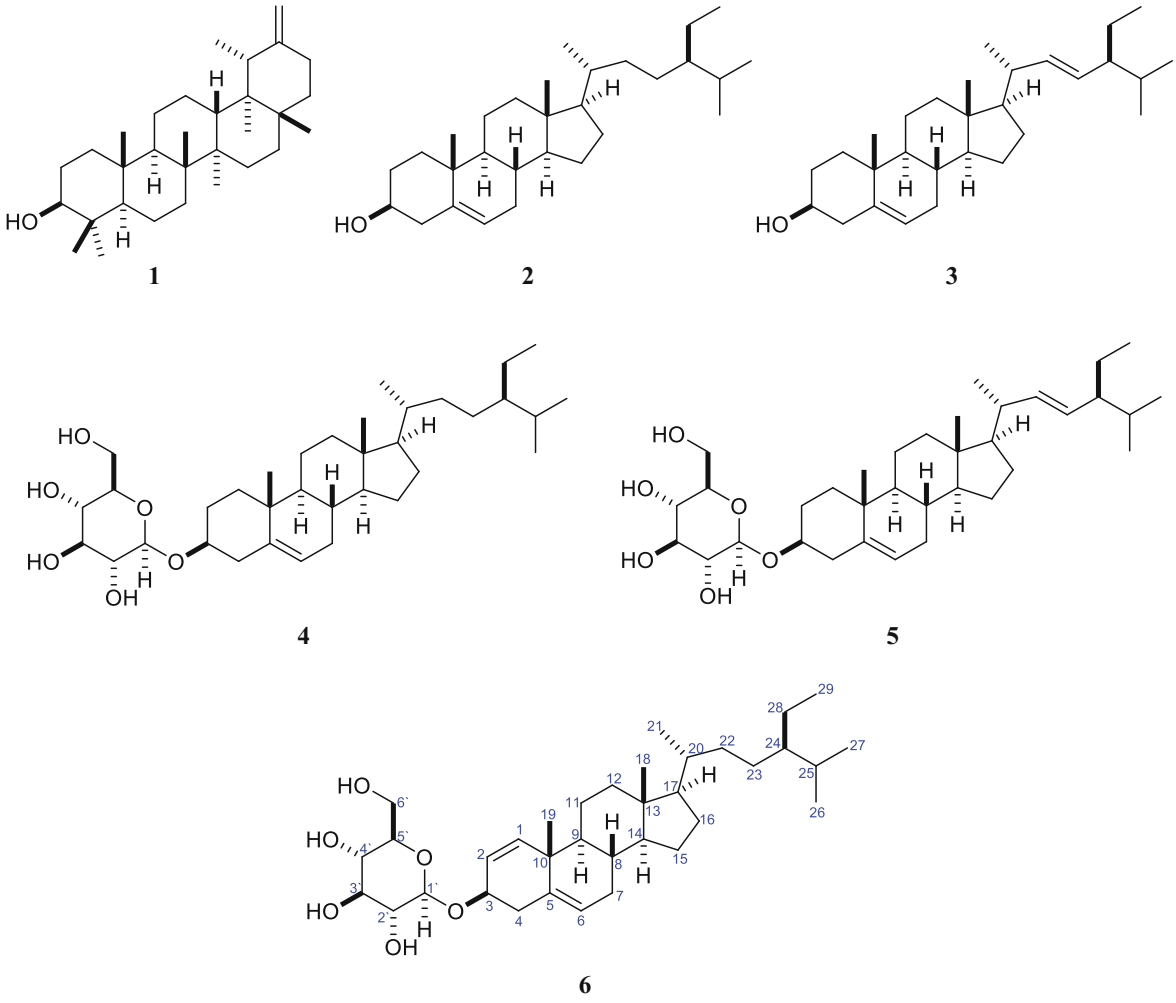

Figure 1: Isolated compounds from *Centaurea pumilio* L. aerial parts.

completely exhausted using DCM followed by methanol. After they were filtered and concentrated under decreased pressure, the combined extracts produced 17 and 44 g of the dichloromethane and methanol extracts, respectively.

The phytochemical investigation of the DCM fraction using different chromatographic techniques led to the isolation of six compounds (namely compounds **1–6**) (Figure 1), and the positive results of the Salkowski's and Liebermann-Burchard's tests indicated their triterpenoid and/or steroidal nature [25]. The structures of the isolated compounds were identified as taraxasterol (**1**) [26], β-sitosterol (**2**) [28], stigmasterol (**3**) [27], stigmasterol-3-*O*-β-D-glucopyranoside (**4**) [28], and stigmasterol-5,22-diene-3-*O*-β-D-glucopyranoside (**5**) [29], which were reported in *C. pumilio* for the first time, whereas compound (**6**) is hereby reported for the first time as being isolated from a natural source. All isolated compounds were identified based on their structures using different physical, chemical, and spectroscopic methods (IR, NMR, and mass spectrometry), in addition to comparison with the published data.

Compound **6** was obtained as a white solid powder, showing a molecular formula $C_{35}H_{58}O_6$ based on a molecular ion peak $[M + H]^+$ at m/z 575.4314 (calcd 575.4312 for $C_{35}H_{59}O_6$) with seven degrees of unsaturation (DBE). The IR spectrum of compound **6** revealed absorption bands at υ_{max} 3,450 and 1,640 cm^{-1} assigned to hydroxyl and olefinic groups, respectively. The compound gave positive Salkowski and Molisch's reactions, indicating its triterpenoid and/or steroidal glycosidic nature.

The ^{1}H-NMR (DMSO-d_6) spectrum of compound (**6**) appeared between δ_H 0.65 and 5.32 ppm and showed six high-intensity peaks for six methyls, including two tertiary methyls at δ_H 0.65 (Me-18) and 0.96 (Me-19); three secondary methyls at δ_H 0.89 (Me-26, Me-27), and 0.89 (Me-21); and one primary methyl at δ_H 0.88 (Me-29); along with one *O*-bearing methine at δ_H 3.45 (H-3), two disubstituted olefinic protons at δ_H 5.14 (H-1), and 4.93 (H-2) and one trisubstituted olefinic proton at δ_H 5.32 (H-6) [28]. An anomeric proton of the sugar moiety was observed at δ_H 4.22 (1H, d, J = 8 Hz), linked with a β-linkage as denoted by the large coupling constant (Table 2).

The ^{13}C-NMR spectrum showed 35 carbons, including six methyls at δ_C 12.1 (CH_3-18), 12.2 (CH_3-29), 19.1 (CH_3-21), 19.3 (CH_3-26), 19.4 (CH_3-27), and 19.6 (CH_3-19). Besides the four methine signals at δ_C 70.6, 77.1, 73.9, and 77.1, corresponding to C-2′, C-3′, C-4′, and C-5′, respectively, an anomeric signal at δ_C 101.2 and one methylene at δ_C 61.5 (C-6′) indicated the presence of a single monosaccharide moiety of α-D-glucopyranoside. The olefinic resonances at δ_C 137.0, 128.7, and 121.7 corresponded to C-1, C-2, and C-6 methine carbons, respectively, in addition to a signal at δ_C 140.8, which corresponded to the C-5 quaternary carbon (Table 2).

Table 2: ^{1}H (500 MHz) and ^{13}C (125 MHz) NMR, CD_3OD spectral data for compound (**6**)

Position	δ_H (*m*, *J* in Hz)	δ_C, mult.
1	5.14 (1H, d, J = 8.4)	137.0, CH
2	4.93 (1H, dd, J = 8.4, 8.4)	128.7, CH
3	3.45 (1H, m)	77.5, CH
4	1.78 (2H, m)	42.0, CH_2
5	—	140.8, C
6	5.32 (1H, d, J = 5.2)	121.7, CH
7	1.23	29.4, CH_2
8	1.48	31.9, CH
9	0.88	50.1, CH
10	—	36.8, C
11	1.40	21.0, CH_2
12	1.81	37.3, CH_2
13	—	39.2, C
14	0.99	56.5, CH
15	1.52	24.3, CH_2
16	1.80	29.2, CH_2
17	1.10	55.9, CH
Me-18	0.65 (3H, s)	12.1, CH_3
Me-19	0.96 (3H, s)	19.6, CH_3
20	1.3	35.9, CH
Me-21	0.89 (3H, d, J = 6.6)	19.1, CH_3
22	1.48	31.8, CH_2
23	1.15	25.9, CH_2
24	0.9	45.6, CH
25	0.82 (1H, d, J = 6.0)	29.2, CH
Me-26	0.89 (3H, d, J = 6.6)	19.3, CH_3
Me-27	0.89 (3H, d, J = 6.6)	19.4, CH_3
28	1.11	23.0, CH_2
Me-29	0.88 (3H, d, J = 6.9)	12.2, CH_3
Sugar moiety		
1′	4.22 (1H, d, J = 8)	101.2, CH
2′	3.02	70.6, CH
3′	3.14	77.1, CH
4′	2.91	73.9, CH
5′	3.14	77.1, CH
6′	3.64	61.5, CH_2

The full assignments of all protons and carbons were performed by ^{1}H-^{13}C HSQC and ^{1}H-^{13}C HMBC, indicating the gross structure of compound **6** as a sterol-3-*O*-glycoside (Figure 2). Key ^{1}H-^{13}C HMBC correlations were observed between H_3-18 and C-13; H_3-19 and C-5, C-9 and C-10; H_3-21 and C-20; H_3-26, H_3-27 and C-25; H_3-29 and C-28. Moreover, key HMBC correlations from H-3 (δ_H 3.45) to C-1 (δ_C 137.0), C-2 (δ_C 128.7), and C-5 (δ_C 140.9) accompanied by HMBC correlations from H_3-19 (δ_H 0.65) to C-1 (δ_C 137.0) and C-5; H-7 (δ_H 1.23) to C-6

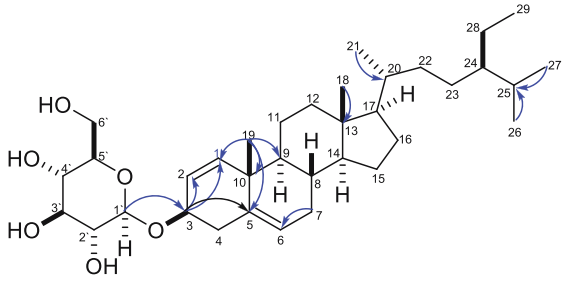

Figure 2: Key ^{1}H-^{13}C HMBC of compound **6**.

(δ_C 121.7) confirmed the olefinic bonds at C-1 and C-5. Furthermore, HMBC correlations between H-1′ (δ_H 4.22) and C-3 (δ_C 77.9) indicated a glycosidic linkage at C-3 (Figure 2). Comparing these spectroscopic results with previous data of identified free aglycone [13], the molecular structure of compound (**6**) was identified as stigmast-1,5-dien-3-*O*-β-D-glucopyranoside, which was isolated for the first time from a natural source.

3.3 Biological activity

Human umbilical vein endothelial cells (HUVEC) have been used as successful models for research on human endothelium. Considering the importance of fibroblast and endothelial cells in wound repair and regeneration, scientific investigations have revealed an increasing interest in regulating their influence on tissue wound closure [30]. Although this model does not represent all endothelial cell types found in an organism, and as the proliferation of HUVEC cells has been correlated with a strong prognosis in the repair and regeneration of wound process, in the present study, we investigated the effects of different concentrations of the isolated compounds on the viability of HUVEC cells using the cell cytotoxicity (MTT) test.

In accordance with the microscopic observations at 72 h post-treatment, the MTT assay of the studied compounds (**1–6**) did not show any sign of cytotoxicity on HUVEC cells, even at the maximal concentrations. Among the compounds, compound (**5**) (stigmasterol-5,22-diene-3-*O*-β-D-glucopyranoside) and compound (**6**) (stigmast-1,5-dien-3-*O*-β-D-glucopyranoside) at 10, 25, and 50 µg/mL doses exhibited low to mild cell proliferative activity (Figure 3); at the maximal tested dose (50 µg/mL), these compounds enhanced HUVEC cell growth by 14 and 16%, respectively (Figure 3).

Phytosterols are a group of natural plant sterols present in vegetables, nuts, and cereals. They are known for their nutritional and therapeutic values [1]. Notably, because humans cannot synthesize phytosterols, they have to obtain them as dietary supplements [31]. *In vitro* and *in vivo* studies have demonstrated that phytosterols and their conjugates, including sitosterol and other derivatives, function as free-radical scavengers and stabilizers of cell membranes by reducing lipid peroxidation and enhancing the activity of antioxidant enzymes [32–34]. Additionally, phytosterols have been demonstrated to improve hepatic and colon metabolisms in mice models [35], as well as to improve colon, ileal, and gallbladder motility. Additional *in vivo* research has shown that stigmasterol

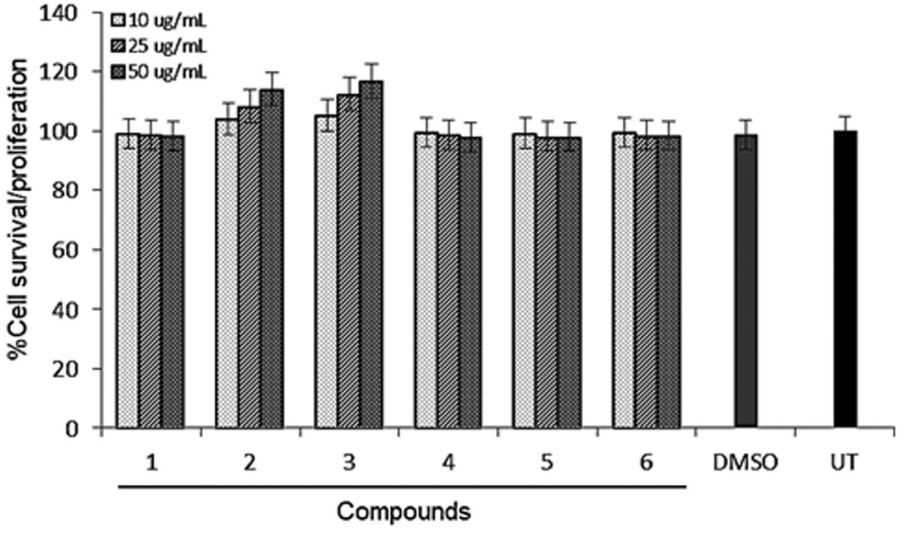

Figure 3: MTT assay showing cell survival or proliferative activities (%) of *C. pumilio* L. derived compounds (**1–6**) at 72 h post-treatment. Vehicle control: DMSO (0.1%); untreated control (UT). Values (*Y*-axis): means of three determinations.

Table 3: Molecular docking parameters for the interaction of compounds **5** and **6** with glycogen synthase kinase-3β (GSK-3β)

Ligand	Δ*G* kcal mol^{-1}	Receptor amino acid
Compound **5**	−7.185	Ile^{62}, Val^{110}, leu^{132}, Tyr^{134}, Arg^{141}, Leu^{188}, Cys^{199}
Compound **6**	−6.303	Ile^{62}, Gln^{185}, Asn^{186}, Leu^{188}
Indirubin-3-monooxime	−5.303	Ile^{62}, Val^{110}, leu^{132}, Asp^{133}, Tyr^{134}, Val^{135}, Leu^{188}, Cys^{199}

can block several pro-inflammatory and matrix-degrading mediators associated with osteoarthritis-induced cartilage deterioration [36]. Accordingly, our data indicated the health-protective effects of stigmasterol-5,22-diene-3-*O*-β-D-glucopyranoside (**5**) and stigmast-1,5-dien-3-*O*-β-D-glucopyranoside (**6**) via their endothelial cell protection and growth stimulation activities, especially in cardiovascular health conditions.

3.4 Molecular docking

To explore the molecular mechanisms underlying the wound-healing activity of the studied compounds, compounds **5** and **6** were docked in the active site of GSK-3β obtained from a protein databank (PDB ID: 1Q41) using Autodock 4.2. The docking energies (kcal/mol) and major

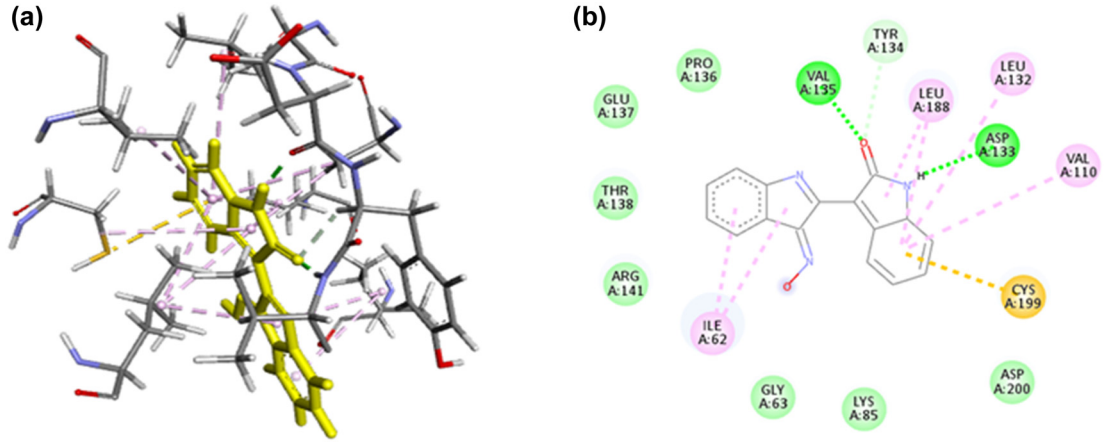

Figure 4: (a) 3D and (b) 2D interactions of the native ligand with GSK-3β. Tyr: Tyrosine; Val: Valine; Leu: Leucine; Ile: Isoleucine; Asp: Aspartic acid; Cys: Cysteine; Arg: Arginine; Glu: Glutamic acid; Pro: Proline; Thr: Threonine; Gly: Glycine; Lys: Lysine.

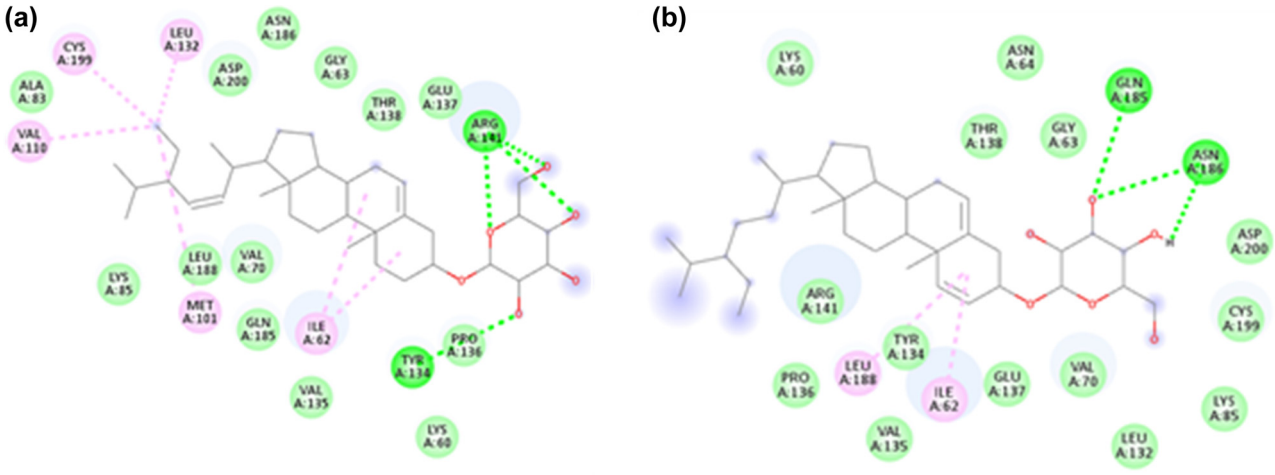

Figure 5: 2D interactions of compounds **5** (a) and **6** (b) with GSK-3β. Ala: Alanine; Tyr: Tyrosine; Val: Valine; Leu: Leucine; Ile: Isoleucine; Asp: Aspartic acid; Asn: Asparagine; Cys: Cysteine; Arg: Arginine; Glu: Glutamic acid; Pro: Proline; Thr: Threonine; Gly: Glycine; Lys: Lysine.

interactions are provided in Table 3 and Figure 4 for the native ligand and studied sterols (**5** and **6**). In this context, it was clear that compounds **5** and **6** displayed some interactions similar to those of indirubin-3-monooxime (native ligand) (Figure 5). We observed that π interactions were formed with amino acid residues Leu^{188} and Ile^{62} in the native ligand as well as in compounds **5** and **6**. In addition, π interactions with Val^{110} and Leu^{132} were observed with the native ligand and compound **5**. Moreover, the native ligand was found to form conventional hydrogen interactions with Val^{135} and Asp^{133}, in addition to van der Waals interactions with Tyr^{134}. Compound **5** was found to form hydrogen interactions with Tyr^{134} and Arg^{141}, whereas compound **6** formed a hydrogen bond with amino acid residues Gln^{185} and Asn^{186}.

Based on our findings, it was evident that compounds **5** and **6** bind to the substrate-binding site of GSK-3β and potentially interact with the key active site residues of the enzyme, forming strong π and hydrogen interactions with the catalytic site residues, revealing lower binding energy (−7.185 and −6.303 kcal/mol, respectively) than that of indirubin-3-monooxime (−5.303 kcal/mol); thus, they could be used as strong natural replacements for GSK-3β inhibitors.

4 Conclusion

Six sterols and triterpenes, including a new compound (**6**), were isolated and identified from the aerial parts of *C. pumilio*. Structural determination was carried out using 1D, 2D NMR, and mass spectroscopic analyses and by comparisons with the published data. All six identified compounds were identified for the first time from the studied plant species. Their cell viability was evaluated using an MTT assay on cultured human primary umbilical vein endothelial cells (HUVEC), revealing that none of the isolated compounds exhibited any sign of cytotoxicity. Furthermore, compounds (**5**) and (**6**) exhibited growth stimulatory actions in HUVEC cells. Finally, molecular docking was performed with glycogen synthase kinase-3β (GSK-3β) to simulate and potentially understand the possible binding interactions underlying the association between our target compounds and GSK-3β essential amino acids to investigate their potential wound healing activity. However, this analysis was not sufficient to decisively discern the mechanism of action of these compounds. Nevertheless, based on the limited evidence, the mechanism of action of these compounds is more likely to involve the action of GSK-3β. Altogether, the data provided in the present study are a contribution to the exploration of structural diversity and biological activity of sterols used for health protection and prevention of cardiovascular diseases.

Abbreviations

DMEM-Glutmax media	DMSO: dimethyl sulfoxide; Dulbecco's modified Eagle medium
HUVEC cells	human primary umbilical vein endothelial cells
MTT assay	3-(4,5-dimethylthiazol-2-yl)-2,5-diphenyltetrazolium bromide
NMR	nuclear magnetic resonance
UPLC-ESI-MS/MS	ultra performance liquid chromatography-electrospray ionization-tandem mass spectrometry

Acknowledgements: The authors express their gratitude to the Princess Nourah bint Abdulrahman University Researchers Supporting Project number (PNURSP2023R3), Princess Nourah bint Abdulrahman University, Riyadh, Saudi Arabia, for funding this work and to Researchers Supporting Project (no. RSP2023R379), King Saud University, Riyadh, Saudi Arabia. The authors also thank Prince Naif Health Research Center, Investigator Support Unit for the language editing service provided.

Funding information: This work was funded by the Princess Nourah bint Abdulrahman University Researchers Supporting Project number (PNURSP2023R3), Princess Nourah bint Abdulrahman University, Riyadh, Saudi Arabia and Researchers Supporting Project number (RSP2023R379), King Saud University, Riyadh, Saudi Arabia.

Author contributions: M.A.A.F, R.O.B and W.M.A.: conceptualization; M.A.A.F, R.O.B, L.H.A., M.K.P., O.A.B. and W.M.A.: data curation; M.A.A.F, R.O.B, M.S.N., O.A.B. and M.K.P.: analysis; L.H.A.: funding acquisition; M.A.A.F, M.K.P. and M.S.A.: investigation; M.A.A.F, R.O.B, O.A.B. and M.S.A.: methodology; M.A.A.F, R.O.B and M.S.N.: resources; M.A.A.F, L.H.A., M.S.A. and W.M.A.: supervision; M.A.A.F, R.O.B, M.S.N., L.H.A., M.K.P. and W.M.A.: writing original draft. All authors shared writing – review, editing, and approval of the final draft.

Conflict of interest: All authors declare that there are no conflicts of interest.

Ethical approval: The conducted research is not related to either human or animal use.

Data availability statement: The data sets generated during and/or analyzed during the current study are available from the corresponding author upon reasonable request.

References

[1] Salehi B, Quispe C, Sharifi-Rad J, Cruz-Martins N, Nigam M, Mishra AP, et al. Phytosterols: from preclinical evidence to potential clinical applications. Front Pharmacol. 2021;11:599959. doi: 10.3389/fphar.2020.599959.

[2] Sharma N, Tan MA, An SSA. Phytosterols: Potential metabolic modulators in neurodegenerative diseases. Int J Mol Sci. 2021;22(22):12255. doi: 10.3390/ijms222212255.

[3] Babu S, Jayaraman S. An update on β-sitosterol: A potential herbal nutraceutical for diabetic management. Biomed Pharmacother. 2020;131:110702. doi: 10.1016/j.biopha.2020.110702.

[4] Eming SA, Krieg T, Davidson JM. Inflammation in wound repair: Molecular and cellular mechanisms. J Invest Dermatol. 2007;127(3):514–25. doi: 10.1038/sj.jid.5700701.

[5] Martin P, Nunan R. Cellular and molecular mechanisms of repair in acute and chronic wound healing. Br J Dermatol. 2015;173(2):370–8. doi: 10.1111/bjd.13954.

[6] Harish BG, Krishna V, Santosh Kumar HS, Khadeer Ahamed BM, Sharath R, Kumara Swamy HM. Wound healing activity and docking of glycogen-synthase-kinase-3-beta-protein with isolated triterpenoid lupeol in rats. Phytomedicine. 2008;15(9):763–7. doi: 10.1016/j.phymed.2007.11.017.

[7] Chen RF, Lin YN, Liu KF, Wang CT, Ramachandran S, Wang CJ, et al. The acceleration of diabetic wound healing by low-intensity extracorporeal shockwave involves in the GSK-3β Pathway. Biomedicines. 2020;9(1):21. doi: 10.3390/biomedicines9010021.

[8] Bruno M, Bancheva S, Rosselli S, Maggio A. Sesquiterpenoids in subtribe *Centaureinae* (Cass.) Dumort (tribe Cardueae, Asteraceae): distribution, (13)C NMR spectral data and biological properties. Phytochemistry. 2013;95:19–93. doi: 10.1016/j.phytochem.2013.07.002.

[9] Formisano C, Rigano D, Senatore F, Bancheva S, Maggio A, Rosselli S, et al. Flavonoids in subtribe *Centaureinae* (Cass.) Dumort. (tribe Cardueae, Asteraceae): distribution and (13)C-NMR spectral data. Chem Biodivers. 2012;9(10):2096–158. doi: 10.1002/cbdv.201100208.

[10] Milošević Ifantis T, Solujić S, Pavlović-Muratspahić D, Skaltsa H. Secondary metabolites from the aerial parts of *Centaurea pannonica* (Heuff.) Simonk. from Serbia and their chemotaxonomic importance. Phytochemistry. 2013;94:159–70. doi: 10.1016/j.phytochem.2013.05.014.

[11] Komilov BD, Eshbakova KA. Flavonoids and sterols of *Centaurea squarrosa*. Chem Nat Compd. 2022;58:746–7. doi: 10.1007/s10600-022-03783-x.

[12] öksüz S, Serin S. Triterpenes of *Centaurea ptosimopappoides*. Phytochemistry. 1997;46(3):545–8. doi: 10.1016/S0031-9422(97)00309-9.

[13] Dumlu MU, Gürkan E. A new active compound from *Centaurea* species. Z Naturforsch C J Biosci. 2006;61(1–2):44–6. doi: 10.1515/znc-2006-1-208.

[14] Abbas AM, Ayed FAA, Sheded MG, Alrumman SA, Radwan TAA, Badry MO. Vegetation analysis and environmental relationships of riverain plants in the aswan reservoir, Egypt. Plants. 2021;10(12):2712. doi: 10.3390/PLANTS10122712.

[15] Mostafa E, Fayed MAA, Radwan RA, Bakr RO. *Centaurea pumilio* L. extract and nanoparticles: A candidate for healthy skin. Colloids Surf B Biointerfaces. 2019;182:110350. doi: 10.1016/j.colsurfb.2019.110350.

[16] Adel R, Gamal A, Al-Gendy AA, Hafez SS. Phytoconstituents profile and UPLC-ESI-MS/MS analysis of *Centaurea pumilio* L. callus culture following elicitation. Asian J Plant Sci. 2021;20:435–49. doi: 10.3923/ajps.2021.435.449.

[17] Naeim H, El-Hawiet A, Abdel Rahman RA, Hussein A, El Demellawy MA, Embaby AM. Antibacterial activity of *Centaurea pumilio* L. root and aerial part extracts against some multidrug resistant bacteria. BMC Complement Med Ther. 2020;20(1):79. doi: 10.1186/s12906-020-2876-y.

[18] Yousif F, Wassel G, Boulos L, Labib T, Mahmoud K, El-Hallouty S, et al. Contribution to *in vitro* screening of Egyptian plants for schistosomicidal activity. Pharm Biol. 2012;50(6):732–9. doi: 10.3109/13880209.2011.625952.

[19] Evans WC. Trease and Evans' pharmacognosy. 6th edn. Philadelphia: W.B. Saunders Company; 2009. p. 1–603

[20] Radhia A, Hanen N, Arfa Abdelkarim B, Mohamed N. Phytochemical screening, antioxidant and antimicrobial activities of *Erodium glaucophyllum* (L.) L'Hérit. J Biomed Sci. 2018;7(4):13–9. doi: 10.4172/2254-609X.100092.

[21] Kokate CK. Practical pharmacognosy. New Delhi: Vallabh Prakarshan; 2001. p. 45–9.

[22] Harborne JB. Phytochemical methods, a guide to modern techniques of plant analysis. 2nd edn. London: Chapman and Hall; 1998. p. 54–84.

[23] Morris GM, Huey R, Lindstrom W, Sanner MF, Belew RK, Goodsell DS, et al. AutoDock4 and AutoDockTools4: Automated docking with selective receptor flexibility. J Comput Chem. 2009;30(16):2785–91. doi: 10.1002/jcc.21256.

[24] Mohammad T, Khan FI, Lobb KA, Islam A, Ahmad F, Hassan MI. Identification and evaluation of bioactive natural products as potential inhibitors of human microtubule affinity-regulating kinase 4 (MARK4). J Biomol Struct Dyn. 2019;37(7):1813–29. doi: 10.1080/07391102.2018.1468282.

[25] Adu JK, Amengor CDK, Kabiri N, Orman E, Patamia SAG, Okrah BK. Validation of a simple and robust liebermann-burchard colorimetric method for the assay of cholesterol in selected milk products in ghana. Int J Food Sci. 2019;2019:9045938. doi: 10.1155/2019/9045938.

[26] Khalilov LM, Khalilova AZ, Shakurova ER, Nuriev IF, Kachala VV, Shashkov AS, et al. PMR and ^{13}C NMR spectra of biologically active compounds. XII. Taraxasterol and its acetate from the aerial part of *Onopordum acanthium*. Chem Nat Compd. 2003;39(3):285–8. doi: 10.1023/A:1025478720459.

[27] Edilu A, Adane L, Woyessa D. *In vitro* antibacterial activities of compounds isolated from roots of *Caylusea abyssinica*. Ann Clin Microbiol Antimicrob. 2015;14:15. doi: 10.1186/s12941-015-0072-6.

[28] Ibraheim ZZ, Ahmed AS, Abdel-Mageed WM. Chemical and biological studies of *Euphorbia aphylla*. J Nat Rem. 2013;13(1):35–45. doi: 10.18311/jnr/2013/116.
[29] Alam MS, Chopra N, Ali M, Niwa M. Oleanen and stigmasterol derivatives from *Ambroma augusta*. Phytochemistry. 1996;41(4):1197–200. doi: 10.1016/0031-9422(95)00774-1.
[30] Rodriguez-Menocal L, Salgado M, Ford D, Van Badiavas E. Stimulation of skin and wound fibroblast migration by mesenchymal stem cells derived from normal donors and chronic wound patients. Stem Cell Transl Med. 2012;1(3):221–9. doi: 10.5966/sctm.2011-0029.
[31] Cabral CE, Klein MRST. Phytosterols in the Treatment of Hypercholesterolemia and prevention of cardiovascular diseases. Arq Bras Cardiol. 2017;109(5):475–82. doi: 10.5935/abc.20170158.
[32] Brüll F, Mensink RP, Plat J. Plant sterols: functional lipids in immune function and inflammation. Clin Lipidol. 2009;4(3):355–65. doi: 10.2217/CLP.09.26.
[33] Nashed B, Yeganeh B, HayGlass KT, Moghadasian MH. Antiatherogenic effects of dietary plant sterols are associated with inhibition of proinflammatory cytokine production in Apo E-KO mice. J Nutr. 2005;135(10):2438–44. doi: 10.1093/jn/135.10.2438.
[34] van Rensburg SJ, Daniels WM, van Zyl JM, Taljaard JJ. A comparative study of the effects of cholesterol, beta-sitosterol, beta-sitosterol glucoside, dehydroepiandrosterone sulphate and melatonin on *in vitro* lipid peroxidation. Metab Brain Dis. 2000;15(4):257–65. doi: 10.1023/a:1011167023695
[35] Iaccarino N, Amato J, Pagano B, Di Porzio A, Micucci M, Bolelli L, et al. Impact of phytosterols on liver and distal colon metabolome in experimental murine colitis model: an explorative study. J Enzyme Inhib Med Chem. 2019;34(1):1041–50. doi: 10.1080/14756366.2019.1611802
[36] Gabay O, Sanchez C, Salvat C, Chevy F, Breton M, Nourissat G, et al. Stigmasterol: a phytosterol with potential anti-osteoarthritic properties. Osteoarthr Cartil. 2010;18(1):106–16. doi: 10.1016/j.joca.2009.08.019.